

Intent-aware Diffusion with Contrastive Learning for Sequential Recommendation

Yuanpeng Qu*
University of Tsukuba
Tsukuba, Ibaraki, Japan
qu@cmu.iit.tsukuba.ac.jp

Hajime Nobuhara
University of Tsukuba
Tsukuba, Ibaraki, Japan
nobuhara@iit.tsukuba.ac.jp

Abstract

Contrastive learning has proven effective in training sequential recommendation models by incorporating self-supervised signals from augmented views. Most existing methods generate multiple views from the same interaction sequence through stochastic data augmentation, aiming to align their representations in the embedding space. However, users typically have specific intents when purchasing items (e.g., buying clothes as gifts or cosmetics for beauty). Random data augmentation used in existing methods may introduce noise, disrupting the latent intent information implicit in the original interaction sequence. Moreover, using noisy augmented sequences in contrastive learning may mislead the model to focus on irrelevant features, distorting the embedding space and failing to capture users' true behavior patterns and intents. To address these issues, we propose **Intent-aware Diffusion with Contrastive Learning for Sequential Recommendation (InDiRec)**. The core idea is to generate item sequences aligned with users' purchasing intents, thus providing more reliable augmented views for contrastive learning. Specifically, InDiRec first performs intent clustering on sequence representations using K-means to build intent-guided signals. Next, it retrieves the intent representation of the target interaction sequence to guide a conditional diffusion model, generating positive views that share the same underlying intent. Finally, contrastive learning is applied to maximize representation consistency between these intent-aligned views and the original sequence. Extensive experiments on five public datasets demonstrate that InDiRec achieves superior performance compared to existing baselines, learning more robust representations even under noisy and sparse data conditions.

CCS Concepts

• **Information systems** → **Recommender systems**.

Keywords

Sequential Recommendation, Contrastive Learning, Diffusion Model, Intent Representation Learning

*Corresponding author. This work was supported by the SPRING program of the Japan Science and Technology Agency (JST) under Grant Number JPMJSP2124.

Permission to make digital or hard copies of all or part of this work for personal or classroom use is granted without fee provided that copies are not made or distributed for profit or commercial advantage and that copies bear this notice and the full citation on the first page. Copyrights for components of this work owned by others than the author(s) must be honored. Abstracting with credit is permitted. To copy otherwise, or republish, to post on servers or to redistribute to lists, requires prior specific permission and/or a fee. Request permissions from permissions@acm.org.

SIGIR '25, Padua, Italy

© 2025 Copyright held by the owner/author(s). Publication rights licensed to ACM.
ACM ISBN 979-8-4007-1592-1/25/07
<https://doi.org/10.1145/3726302.3730010>

ACM Reference Format:

Yuanpeng Qu and Hajime Nobuhara. 2025. Intent-aware Diffusion with Contrastive Learning for Sequential Recommendation. In *Proceedings of the 48th International ACM SIGIR Conference on Research and Development in Information Retrieval (SIGIR '25)*, July 13–18, 2025, Padua, Italy. ACM, New York, NY, USA, 10 pages. <https://doi.org/10.1145/3726302.3730010>

1 Introduction

Sequential recommendation (SR), an essential task in recommender systems, has been widely adopted across various online platforms. It aims to predict the next item a user is likely to interact with based on his/her historical interaction sequence [36, 45]. A key challenge in SR is data sparsity, as limited user-item interaction records make it difficult to capture deep behavior patterns and long-term dependencies in sequences [24]. Recently, contrastive learning for SR has gained substantial attention due to its effectiveness in addressing this challenge [39]. By leveraging augmented views of user interaction sequences, contrastive learning enables the model to learn more accurate and robust representations, improving its ability to handle data sparsity.

To implement contrastive learning in SR, existing methods [3, 22, 24, 25, 42, 43] primarily perform data augmentation on the original interaction sequence to construct multiple views and maximize representation agreement between different views. These methods generally fall into three categories: (1) Data-level methods [3, 22, 42, 46] generate different views by applying random augmentation to items in the original sequence (e.g. deletion, replacement, masking, or cropping) to enhance representation learning in contrastive frameworks. (2) Model-level methods [25, 43] generate augmented views by randomly applying dropout or masking to neurons in neural network layers, while preserving the semantics of the original sequence. (3) Mixup-level methods [24, 47] apply the former to generate different views, followed by the latter to construct more informative and diverse contrastive pairs.

While most above methods [3, 22, 24, 25, 42, 46] have partially alleviated the data sparsity issue, their reliance on random augmentation introduces considerable uncertainty. This often leads to the neglect of users' latent intents, making them difficult for models to capture. To address these issues and better capture users' latent intents, it is essential to tackle the following challenges. First, latent intents are abstract and lack explicit labels, making them difficult to materialize. They can only be inferred from limited user interaction sequences. As shown in Figure 1, random data augmentation can disrupt the original sequence semantics, potentially altering the underlying intent. Besides, items driven by the same intent in a user's interaction sequence may appear non-contiguously. For instance, in Figure 1, Bob purchased a keyboard, mouse, and monitor to assemble a computer. Although the monitor was bought at a different

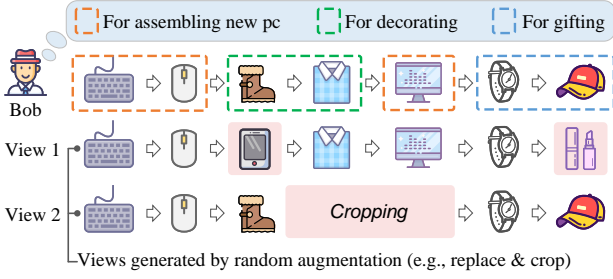


Figure 1: An example illustrates that random data augmentation may disrupt the semantic consistency of users' purchasing intents, affecting the model's understanding.

time, it still reflects the same intent. Ignoring such latent factors may prevent the model from generating positive views with consistent semantics to the original sequence, limiting its ability to learn intent representations and resulting in performance degradation.

Given these challenges, a natural question arises: How can we effectively generate intent-aware augmented views for contrastive learning? Our basic idea is to learn the intent representation of the target sequence, derive its conditional distribution, and generate a new sequence representation sharing the same intent for contrastive learning. To this end, we propose the **Intent-aware Diffusion with contrastive learning for sequential Recommendation (InDiRec)**. By leveraging the diffusion model's superior capability in learning data distributions and performing strong controllable conditional generation [10, 18], InDiRec captures the underlying distribution of the target sequence's intent representation and samples intent-aware positive augmented views. Specifically, we use a dynamic segmentation approach to split the original training sequence into multiple prefix-like subsequences. We then encode these subsequences with a sequence encoder and cluster the resulting representations to derive intent prototypes, ensuring that items scattered across different subsequences but sharing the same intent are effectively aggregated. We refer to this entire process as intent-guided signal construction. Next, for a given target sequence, we first locate its corresponding intent prototype and use a Transformer-based encoder [13] to retrieve other sequence representations sharing the same intent. These representations act as conditional input to guide the diffusion model. We then feed the target sequence into this intent-aware diffusion model to generate an augmented view that preserves the same intent. This augmented view is treated as a positive sample in contrastive learning alongside the original sequence representation. Moreover, unlike other diffusion-based SR models [19, 44], InDiRec applies its distribution learning and sampling during training, achieving comparable faster inference. Our main contributions are summarized as follows:

- We propose InDiRec¹, a novel approach that first leverages user intent as guidance to generate semantically consistent augmented views for contrastive learning in the SR task.
- We introduce intent-aware diffusion to sample meaningful augmented views from the learned intent distribution, effectively addressing challenges caused by random augmentation.

¹Our code is available at <https://github.com/qyp9909/InDiRec>.

- Extensive experiments on five public datasets further validate the effectiveness of InDiRec, demonstrating its ability to alleviate data sparsity while improving performance and robustness.

2 Preliminary

2.1 Problem Definition

Sequential recommendation (SR) is designed to predict and recommend the next item by learning from the target user's historical interactions. Let \mathcal{U} and \mathcal{I} represent the sets of users and items, respectively. Each user $u \in \mathcal{U}$ has a chronological interaction sequence $S^u = [v_1^u, v_2^u, \dots, v_{|S^u|}^u]$, where $v_t^u \in \mathcal{I}$ ($1 \leq t \leq |S^u|$) denotes the item interacted by u at step t , and $|S^u|$ represents the length of u 's interaction sequence. The goal of SR is to predict the next item u may interact with at step t , formulated as:

$$\arg \max_{v \in \mathcal{I}} P(v_{|S^u|+1}^u = v | S^u) \quad (1)$$

2.2 Diffusion Models

To better understand the proposed method, we briefly introduce the basics of diffusion models based on the DDPM [10] framework before presenting InDiRec. Typically, diffusion models consist of a forward process and a reverse process. In the forward process, starting from the original data samples $\mathbf{x}_0 \sim q(\mathbf{x}_0)$, noise is gradually added over T steps until the data transforms into standard Gaussian noise $\mathbf{x}_T \sim \mathcal{N}(0, \mathbf{I})$. The transition from \mathbf{x}_{t-1} to \mathbf{x}_t is given by:

$$q(\mathbf{x}_t | \mathbf{x}_{t-1}) = \mathcal{N}(\mathbf{x}_t; \sqrt{1 - \beta_t} \mathbf{x}_{t-1}, \beta_t \mathbf{I}), \quad (2)$$

where $\{\beta_t\}_{t=1}^T$ is the variance schedule at time step t . Based on the properties of independent Gaussian distributions and the reparameterization trick, \mathbf{x}_t can be directly calculated from \mathbf{x}_0 :

$$q(\mathbf{x}_t | \mathbf{x}_0) = \mathcal{N}(\mathbf{x}_t; \sqrt{\bar{\alpha}_t} \mathbf{x}_0, (1 - \bar{\alpha}_t) \mathbf{I}), \quad (3)$$

where $\alpha_t = 1 - \beta_t$ and $\bar{\alpha}_t = \prod_{s=1}^t \alpha_s$. In this way, we can reparameterize $\mathbf{x}_t = \sqrt{\bar{\alpha}_t} \mathbf{x}_0 + \sqrt{1 - \bar{\alpha}_t} \epsilon$, $\epsilon \sim \mathcal{N}(0, \mathbf{I})$.

The reverse process aims to gradually reconstruct the original data \mathbf{x}_0 from standard Gaussian noise \mathbf{x}_T over T steps. A neural network parameterized by θ predicts the distribution of the reverse transition from \mathbf{x}_t to \mathbf{x}_{t-1} , which can be formulated as follows:

$$p_\theta(\mathbf{x}_{t-1} | \mathbf{x}_t) = \mathcal{N}(\mathbf{x}_{t-1}; \mu_\theta(\mathbf{x}_t, t), \Sigma_\theta(\mathbf{x}_t, t)), \quad (4)$$

where $\mu_\theta(\mathbf{x}_t, t)$ and $\Sigma_\theta(\mathbf{x}_t, t)$ represent the mean and variance of this distribution, respectively.

To train diffusion models, the variational lower bound can be used to minimize $-\log p_\theta(\mathbf{x}_0)$. The loss function is defined as:

$$\begin{aligned} \mathcal{L} = \mathbb{E}_{q(\mathbf{x}_0)} [-\log p_\theta(\mathbf{x}_0)] &\leq \mathbb{E}_q [D_{KL}(q(\mathbf{x}_T | \mathbf{x}_0) || p_\theta(\mathbf{x}_T))] \\ &+ \sum_{t=2}^T D_{KL}(q(\mathbf{x}_{t-1} | \mathbf{x}_t, \mathbf{x}_0) || p_\theta(\mathbf{x}_{t-1} | \mathbf{x}_t)) - \log p_\theta(\mathbf{x}_0 | \mathbf{x}_1). \end{aligned} \quad (5)$$

DDPM further simplifies the t -th term of the training objective, deriving a mean-squared error loss as follows:

$$\mathcal{L}_t^{\text{simple}} = \mathbb{E}_{q(\mathbf{x}_t | \mathbf{x}_0)} [\|\tilde{\mu}_t(\mathbf{x}_t, \mathbf{x}_0) - \mu_\theta(\mathbf{x}_t, t)\|^2], \quad (6)$$

where $\tilde{\mu}_t(\mathbf{x}_t, \mathbf{x}_0)$ represents the mean of the posterior distribution $q(\mathbf{x}_{t-1} | \mathbf{x}_t, \mathbf{x}_0)$, which can be computed when \mathbf{x}_0 is determined, while $\mu_\theta(\mathbf{x}_t, t)$ denotes the predicted mean of $p_\theta(\mathbf{x}_{t-1} | \mathbf{x}_t)$ obtained via a neural network parameterized by θ .

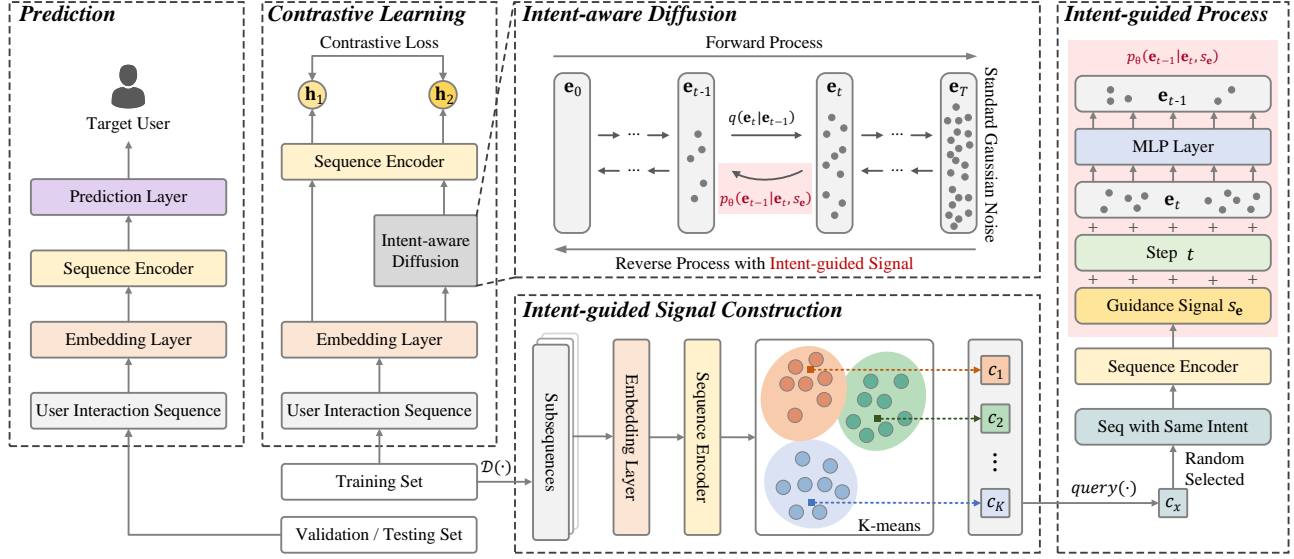


Figure 2: Overview of our InDiRec. InDiRec first performs Intent-guided Signal Construction on training sequences, where c_x denotes the intent prototype. It then generates positive augmented views via Intent-aware Diffusion guided by s_e . Finally, the views and the original sequence are encoded into h_1 and h_2 , which are optimized through contrastive learning.

3 Methodology

The overview of the proposed method, InDiRec, is illustrated in Figure 2. It consists of three main components: intent-guided signal construction, intent-aware diffusion, and model training & prediction. In this section, we first introduce the method for dividing subsequences and constructing intent-guided signals through intent clustering on their representations. Next, we detail the intent-aware diffusion process and explain how intent-guided signals direct diffusion to generate augmented views aligned with the original sequence’s intent. Finally, we describe the training and prediction process of InDiRec.

3.1 Intent-guided Signal Construction

3.1.1 Dynamic Incremental Prefix Segmentation $\mathcal{D}(\cdot)$ for modeling intent. To learn representations of items that are interacted with at different time steps but share the same latent intent, we first divide the original sequence into multiple subsequences using $\mathcal{D}(\cdot)$ [30]. For an interaction sequence $S^u = [v_1^u, v_2^u, \dots, v_{|S^u|}^u]$ from training set, $\mathcal{D}(\cdot)$ is defined as follows:

$$\mathcal{D}(S^u) = \begin{cases} \{[v_1^u, v_2^u, \dots, v_m^u], \dots, [v_1^u, v_2^u, \dots, v_{|S^u|}^u]\}, & |S^u| \leq n, \\ \{\mathcal{D}(S_{1:n}^u), [v_2^u, \dots, v_{n+1}^u], \dots, \\ [v_{|S^u|-(n-1)}^u, \dots, v_{|S^u|}^u]\}, & |S^u| > n, \end{cases} \quad (7)$$

where the length of each subsequence falls within the interval $[m, n]$, ensuring that the subsequences provide sufficient semantic information while avoiding excessive computational overhead.

3.1.2 Embedding layer. First, we embed all items into a shared space, resulting in the item embedding matrix $\mathbf{M} \in \mathbb{R}^{|I| \times d}$. For a given input sequence S^u , we compute its embedding as $\mathbf{e}^u = [e_1^u, e_2^u, \dots, e_n^u]$, where $\mathbf{e}^u \in \mathbb{R}^{n \times d}$ and n represents the length of

the sequence. For a given user, we omit u and denote \mathbf{e}^u as \mathbf{e} to make the following equations more intuitive. Next, the input vector $\mathbf{h}^0 = \mathbf{e} + \mathbf{p}$ is obtained by adding positional embeddings $\mathbf{p} \in \mathbb{R}^{n \times d}$ to item embeddings.

3.1.3 Sequence Encoder. After obtaining the embedding \mathbf{h}^0 , we input it into an L -layer Transformer-based sequential model (e.g., SASRec [13]), denoted as $\text{Trans}(\cdot)$, which serves as the backbone model to learn sequence representations. It is defined as follows:

$$\mathbf{h}^L = \text{Trans}(\mathbf{h}^0). \quad (8)$$

Here, the hidden states of the last layer are denoted as $\mathbf{h}^L \in \mathbb{R}^{n \times d}$, where the final vector $\mathbf{h}_n^L \in \mathbb{R}^d$ represents the entire user sequence and is used as the sequence’s intent representation.

3.1.4 Intent Representation Learning. Since the same latent intent can arise from subsequences in different categories or contexts (e.g., for a gifting intent, one user may buy clothes while another buys books) [23], we assume there are K categories of intents. Building on this assumption, we aggregate items with the same intent across overlapping subsequences to capture users’ intents better. After computing all subsequences’ intent representations using Eq.(8), we apply the K-means clustering algorithm [12] to construct the intent-guided signal, which is formulated as follows:

$$\text{minimize}_{\{c_j\}_{j=1}^K} \sum_{i=1}^{\mathcal{T}} \min_{j \in \{1, \dots, K\}} \|\mathbf{h}_i - c_j\|^2. \quad (9)$$

Here, \mathbf{h}_i denotes the intent representation of each subsequence in the training set \mathcal{T} . The cluster centers $\mathbf{C} = \{c_j\}_{j=1}^K$ are the intent prototypes, where $c_j \in \mathbb{R}^d$ represents the j -th prototype.

With the intent-guided signal constructed, we can use $\text{query}(\cdot)$ to find the corresponding intent prototype for any input sequence’s

intent representation \mathbf{h}' , which is formulated as:

$$\text{query}(\mathbf{h}') = \arg \min_{j \in \{1, \dots, K\}} \|\mathbf{h}' - c_j\|^2. \quad (10)$$

3.2 Intent-aware Diffusion

Existing methods overlook the intent information embedded in user interaction sequences, while random data augmentation further disrupts the semantics of items interacted with at different times but sharing the same intent. This makes it challenging to construct reasonable augmented views for contrastive learning. In contrast, leveraging the stability and controllability of diffusion models, we use intent information as guidance to generate augmented views aligned with the target sequence's intent, referred to as intent-aware diffusion. Similar to DDPM [10], intent-aware diffusion consists of a forward process and a reverse process, which will be detailed in the following sections.

3.2.1 Forward Process. In the forward process, given the embedding of a target interaction sequence \mathbf{e}_0 as input, intent-aware diffusion gradually adds noise to it following a variance schedule $[\beta_1, \beta_2, \dots, \beta_T]$, until it becomes standard Gaussian noise \mathbf{e}_T . Similar to Eq.(2), the forward process at step t is defined as:

$$q(\mathbf{e}_t | \mathbf{e}_{t-1}) = \mathcal{N}(\mathbf{e}_t; \sqrt{1 - \beta_t} \mathbf{e}_{t-1}, \beta_t \mathbf{I}). \quad (11)$$

3.2.2 Reverse Process with Intent-guided Signal. In the reverse process, we use Eq.(9) to construct the intent-guided signal that directs the diffusion model in generating intent-aligned augmented views. Specifically, we first obtain the representation \mathbf{h}_e of the target interaction sequence using Eq.(8), then locate its intent prototype c_e via Eq.(10). A sequence with the same intent is randomly selected from c_e to generate the guidance signal s_e through Eq.(8). Finally, s_e is used as a condition to guide the reverse process in producing intent-aligned sequence representations. The formula at step t is as follows:

$$p_\theta(\mathbf{e}_{t-1} | \mathbf{e}_t, s_e) = \mathcal{N}(\mathbf{e}_{t-1}; \mu_\theta(\mathbf{e}_t, s_e, t), \Sigma_\theta(\mathbf{e}_t, s_e, t)). \quad (12)$$

Here, $\mu_\theta(\mathbf{e}_t, s_e, t)$ is learned by a neural network parameterized by θ , where we use an MLP for implementation. To simplify calculation, $\Sigma_\theta(\mathbf{e}_t, s_e, t)$ is set as a time-dependent constant.

3.2.3 Training Phase. To train intent-aware diffusion, we introduce the intent-guided signal into Eq.(5) to define the optimization objective at step t :

$$\mathcal{L}_t = D_{KL}(q(\mathbf{e}_{t-1} | \mathbf{e}_t, \mathbf{e}_0) || p_\theta(\mathbf{e}_{t-1} | \mathbf{e}_t, s_e)). \quad (13)$$

Based on Bayes' theorem, $q(\mathbf{e}_{t-1} | \mathbf{e}_t, \mathbf{e}_0)$ can be approximated as:

$$q(\mathbf{e}_{t-1} | \mathbf{e}_t, \mathbf{e}_0) = \mathcal{N}(\mathbf{e}_{t-1}; \tilde{\mu}_t(\mathbf{e}_t, \mathbf{e}_0, t), \tilde{\sigma}_t^2 \mathbf{I}), \text{ where} \quad (14)$$

$$\begin{cases} \tilde{\mu}_t(\mathbf{e}_t, \mathbf{e}_0, t) = \frac{\sqrt{\alpha_t}(1 - \tilde{\alpha}_{t-1})}{1 - \tilde{\alpha}_t} \mathbf{e}_t + \frac{\sqrt{\tilde{\alpha}_{t-1}}(1 - \alpha_t)}{1 - \tilde{\alpha}_t} \mathbf{e}_0, \\ \tilde{\sigma}_t^2 = \frac{1 - \tilde{\alpha}_{t-1}}{1 - \tilde{\alpha}_t} \beta_t. \end{cases} \quad (15)$$

At this point, we obtain the mean and variance of $q(\mathbf{e}_{t-1} | \mathbf{e}_t, \mathbf{e}_0)$. Note that $\mathbf{e}_t = \sqrt{\alpha_t} \mathbf{e}_0 + \sqrt{1 - \alpha_t} \epsilon$, $\epsilon \sim \mathcal{N}(0, \mathbf{I})$. Following DDPM, we directly set $\Sigma_\theta(\mathbf{e}_t, s_e, t) = \tilde{\sigma}_t^2 \mathbf{I}$ to simplify training calculations. Similar to Eq.(14) and Eq.(15), we apply another reparameterization to p_θ to derive its mean $\mu_\theta(\mathbf{e}_t, s_e, t)$, which is expressed as follows:

$$\mu_\theta(\mathbf{e}_t, s_e, t) = \frac{\sqrt{\alpha_t}(1 - \tilde{\alpha}_{t-1})}{1 - \tilde{\alpha}_t} \mathbf{e}_t + \frac{\sqrt{\tilde{\alpha}_{t-1}}(1 - \alpha_t)}{1 - \tilde{\alpha}_t} f_\theta(\mathbf{e}_t, s_e, t), \quad (16)$$

where $f_\theta(\mathbf{e}_t, s_e, t)$ represents the intent-aware sequence representation predicted based on \mathbf{e}_t , s_e and t , implemented using an MLP, as shown on the right side of Figure 2.

Therefore, the loss function at step t (Eq. (13)) can be further simplified via Eq.(6), Eq.(15), and Eq.(16) [18], formulated as follows:

$$\begin{aligned} \mathcal{L}_t^{\text{diff}} &= \mathbb{E}_{\mathbf{e}_0, \mathbf{e}_t} [\|\tilde{\mu}_t(\mathbf{e}_t, \mathbf{e}_0, t) - \mu_\theta(\mathbf{e}_t, s_e, t)\|^2] \\ &= \mathbb{E}_{\mathbf{e}_0, \mathbf{e}_t} \left[\left\| \frac{\sqrt{\tilde{\alpha}_{t-1}}(1 - \alpha_t)}{1 - \tilde{\alpha}_t} (\mathbf{e}_0 - f_\theta(\mathbf{e}_t, s_e, t)) \right\|^2 \right] \\ &\propto \mathbb{E}_{\mathbf{e}_0, \mathbf{e}_t} [\|\mathbf{e}_0 - f_\theta(\mathbf{e}_t, s_e, t)\|^2], \end{aligned} \quad (17)$$

where \mathbf{e}_0 represents the embedding of the input target interaction sequence. Therefore, the generated sequence representation is optimized using Eq.(17) to align its intent in the embedding space.

3.2.4 Intent-aligned View Generation Phase. To achieve stronger control over the intent-guided signal s_e and generate views more closely aligned with the intent, we adopt a classifier-free guidance scheme in both the training and generation phases [11]. During training, s_e is randomly replaced with an empty condition token ξ allowing the model to learn both conditional and unconditional predictions [6]. During generation, f_θ is modified as follows:

$$\hat{f}_\theta(\mathbf{e}_t, s_e, t) = (1 + \omega) f_\theta(\mathbf{e}_t, s_e, t) - \omega f_\theta(\mathbf{e}_t, \xi, t), \quad (18)$$

where ω is the guidance scale that controls the strength of the guidance signal. Finally, intent-aligned augmented view $\hat{\mathbf{e}}_0$ is obtained by performing T -step sampling from the learned distribution p_θ . The sampling process at step t is expressed as follows:

$$\mathbf{e}_{t-1} = \frac{\sqrt{\alpha_t}(1 - \tilde{\alpha}_{t-1})}{1 - \tilde{\alpha}_t} \mathbf{e}_t + \frac{\sqrt{\tilde{\alpha}_{t-1}}(1 - \alpha_t)}{1 - \tilde{\alpha}_t} \hat{f}_\theta(\mathbf{e}_t, s_e, t) + \sigma_t \epsilon, \quad (19)$$

where $\epsilon \sim \mathcal{N}(0, \mathbf{I})$.

3.3 Intent-aware Contrastive Learning

The goal of intent-aware diffusion is to generate augmented views that share the same intent as the target sequence. To maximize the intent consistency between the generated view and the target interaction sequence in the representation space, InDiRec inputs the embedding of the target sequence \mathbf{e}_0 and the embedding of the generated view $\hat{\mathbf{e}}_0$ into a sequence encoder (Eq.(8)) to obtain representations \mathbf{h}_1 and \mathbf{h}_2 . Contrastive learning is then applied to bring the two intent representations closer in the representation space [2]. The contrastive loss is formulated as follows:

$$\mathcal{L}_{\text{cl}} = \mathcal{L}_c(\mathbf{h}_1, \mathbf{h}_2) + \mathcal{L}_c(\mathbf{h}_2, \mathbf{h}_1), \text{ where} \quad (20)$$

$$\mathcal{L}_c(\mathbf{z}_1, \mathbf{z}_2) = -\log \frac{\exp(\text{sim}(\mathbf{z}_1, \mathbf{z}_2)/\tau)}{\exp(\text{sim}(\mathbf{z}_1, \mathbf{z}_2)/\tau) + \sum_{\mathbf{z} \in \eta} \exp(\text{sim}(\mathbf{z}_1, \mathbf{z})/\tau)}.$$

Here, $(\mathbf{z}_1, \mathbf{z}_2)$ are the embeddings of a pair of positive samples, $\text{sim}(\cdot)$ denotes the inner product of vectors, τ is the temperature parameter and η is the set of negative samples in the mini-batch, excluding those that share the same intent cluster as the anchor, in order to reduce the impact of false negatives [3].

3.4 Prediction Layer

Similar to many SR models, we use the inner product to compute the similarity between the intent-aware representation \mathbf{h}^u and the

item embedding vectors \mathbf{M} , estimating the probability of the next item that user u may interact with, as formulated below:

$$\mathbf{r} = \text{softmax}(\mathbf{h}^u \mathbf{M}^\top), \quad (21)$$

where $\mathbf{r} \in \mathbb{R}^{|\mathcal{I}|}$ denotes the predicted probability distribution of all items. We minimize the cross-entropy loss to align \mathbf{r} with the ground truth item $g \in \mathcal{I}$, which is formulated as follows:

$$\mathcal{L}_{\text{rec}} = -1 * \mathbf{r}[g] + \log \left(\sum_{i \in \mathcal{I}} \exp(\mathbf{r}[i]) \right). \quad (22)$$

3.5 Multi-task Learning

Since intent-aware diffusion, contrastive learning, and the prediction layer share the same representation space with item embeddings, we adopt a multi-task learning paradigm to jointly optimize them for optimal performance. The joint objective function is formulated as follows:

$$\mathcal{L} = \mathcal{L}_{\text{rec}} + \gamma \mathcal{L}_{\text{cl}} + \lambda \mathcal{L}_{\text{diff}}, \quad (23)$$

where γ and λ are hyperparameters determining the weights of contrastive learning and the intent-aware diffusion, respectively. Note that Eq.(17) computes the loss of diffusion at step t , while $\mathcal{L}_{\text{diff}}$ represents the cumulative loss across all T steps of the sampling process. Algorithm 1 shows the details of InDiRec’s training phase.

Algorithm 1 The InDiRec Algorithm

Input: Training set $\{S^u\}_{u=1}^{|\mathcal{U}|}$, sequence encoder $\text{Trans}(\cdot)$ with \mathcal{H} , hyper-parameters K, λ, γ , diffusion steps T , batch size B .
Output: Optimized θ for $\text{Trans}(\cdot)$ to make next item prediction.

- 1: Split $\{S^u\}_{u=1}^{|\mathcal{U}|}$ into multiple subsequences via Eq. (7).
- 2: **while** $\text{epoch} \leq \text{MaxTrainEpoch}$ **do**
- 3: Update intent prototype representation with K via Eq. (9).
- 4: **for** a minibatch $\{S^u\}_{u=1}^B$ with $u \in \{1, 2, \dots, B\}$ **do**
- 5: Query the intent prototype c of an input S^u via Eq. (10).
- 6: Intent-guided Signal $s_e = \text{Trans}(\text{RandomSample}(c))$
- 7: Add noise to S^u ’s embedding \mathbf{e}_0 in T steps via Eq. (11).
- 8: Denoise $\mathbf{e}_T \sim \mathcal{N}(0, \mathbf{I})$ with s_e in T steps via Eq. (12).
- 9: Calculate $\mathcal{L}_{\text{diff}}$ via Eq. (17).
- 10: Sample an augmented view $\hat{\mathbf{e}}_0$ in T steps via Eq. (19).
- 11: $\mathbf{h}_1 = \text{Trans}(\mathbf{e}_0)$, $\mathbf{h}_2 = \text{Trans}(\hat{\mathbf{e}}_0)$
- 12: Calculate \mathcal{L}_{cl} with \mathbf{h}_1 and \mathbf{h}_2 via Eq. (20).
- 13: //joint Optimization.
- 14: $\mathcal{L} = \mathcal{L}_{\text{rec}} + \gamma \mathcal{L}_{\text{cl}} + \lambda \mathcal{L}_{\text{diff}}$
- 15: Update network $\text{Trans}(\cdot)$ with θ to minimize \mathcal{L} .
- 16: **end for**
- 17: **end while**

4 Experiments

4.1 Experimental Settings

4.1.1 Datasets. We conducted extensive experiments on five real-world public datasets. The Beauty, Sports, Toys, and Video datasets are from different categories of the world’s largest e-commerce platform Amazon² reviews. The ML-1M from Movielens³ is a dataset

²<https://jmcauley.ucsd.edu/data/amazon/>

³<https://grouplens.org/datasets/movielens/>

Table 1: Statistical details of all datasets after preprocessing.

Datasets	Beauty	Sports	Toys	Video	ML-1M
# Users	22,363	35,598	19,412	31,013	6,041
# Items	12,101	18,357	11,924	23,715	3,417
# Avg. Length	8.9	8.3	8.6	9.3	165.5
# Actions	198,502	296,337	167,597	28,9305	999,611
Sparsity	99.93%	99.95%	99.93%	99.96%	95.16%

containing one million movie ratings and is widely used for evaluating recommender systems. We preprocess the data following [42, 46], sorting each user’s interactions in chronological order and retaining only users that have at least five interactions. The statistics of all datasets are summarized in Table 1.

4.1.2 Evaluation Metrics. We evaluate InDiRec using two widely adopted top- k metrics: Hit Rate (HR) and Normalized Discounted Cumulative Gain (NDCG). In this work, we report $\text{HR}@k$ and $\text{NDCG}@k$ (ND@ k) with $k \in \{5, 20\}$, and evaluate the model by ranking all items without negative sampling [16]. Following the leave-one-out strategy, the last two items of a sequence are used for validation and testing, while the rest are used for training.

4.1.3 Baseline Methods. To evaluate the effectiveness of InDiRec, we compare it with the following three categories of baselines:

- **General models:** **BPR-MF** [26] uses the Bayesian Personalized Ranking loss to optimize a matrix factorization model. **GRU4Rec** [9] employs GRU to model user sequential patterns in session-based recommendation. **SASRec** [13] is a pioneering work that applies the attention mechanism to modeling user sequences, significantly enhancing SR. **BERT4Rec** [28] introduces a bidirectional Transformer [5, 34] and adopts the Cloze task to capture latent relationships between items and sequences.
- **Contrastive learning-based SR models:** **CL4SRec** [42] is the first to apply data augmentation and contrastive learning to SR, effectively reducing the data sparsity problem. **ICLRec** [3] clusters the intents in user interaction sequences and integrates them into the model through contrastive learning. **IOCRec** [17] employs intent-level contrastive learning to mitigate the noise introduced by data augmentation. **MCLRec** [24] combines model-level augmentation with data-level augmentation to reduce augmentation noise and optimizes the model via meta-learning. **DuoRec** [25] first introduces model-level augmentation to SR and employs a supervised sampling strategy to generate positive samples.
- **Diffusion-based SR models:** **DiffuASR** [21] first generates items using a diffusion model and concatenates them with the raw sequence to form an augmented sequence, which is then used for prediction and recommendation through a general SR model (e.g., BERT4Rec). **DreamRec** [44] directly generates the next item based on users’ historical interaction sequences using a diffusion model with a classifier-free guidance scheme. **CaDiRec** [4] generates context-aware augmented views using a conditional diffusion model and optimizes the model through contrastive learning. **DiffuRec** [19] first introduces diffusion models in SR to transform and reconstruct item representations with uncertainty injection based on historical behaviors.

Table 2: Performance comparison across five datasets. The best results are highlighted in bold, the second-best are underlined, and "Improv." denotes the relative improvement (%) over the second-best method. (p -value<0.05 with paired t-tests).

Dataset	Metric	BPR-MF	GRU4Rec	SASRec	BERT4Rec	CL4SRec	ICLRec	IOCR	MCLRec	DuoRec	DiffuASR	DreamRec	CaDiRec	DiffuRec	InDiRec	Improv.
Beauty	HR@5	0.0176	0.0182	0.0380	0.0363	0.0407	0.0496	0.0508	0.0526	<u>0.0557</u>	0.0425	0.0448	0.0484	0.0543	0.0686	23.16%
	HR@20	0.0480	0.0477	0.0884	0.0992	0.0997	0.1063	0.1146	0.1191	<u>0.1205</u>	0.0989	0.1020	0.1026	0.1109	0.1303	8.13%
	ND@5	0.0103	0.0112	0.0243	0.0221	0.0282	0.0325	0.0311	0.0336	0.0350	0.0269	0.0283	0.0305	<u>0.0399</u>	0.0488	22.31%
	ND@20	0.0179	0.0188	0.0382	0.0396	0.0420	0.0484	0.0487	0.0524	0.0535	0.0430	0.0462	0.0463	<u>0.0554</u>	0.0662	19.49%
Sports	HR@5	0.0120	0.0162	0.0218	0.0217	0.0211	0.0247	0.0294	0.0312	<u>0.0319</u>	0.0232	0.0243	0.0267	0.0273	0.0378	18.50%
	HR@20	0.0343	0.0421	0.0493	0.0604	0.0546	0.0579	0.0677	<u>0.0721</u>	0.0717	0.0608	0.0636	0.0622	0.0587	0.0787	9.15%
	ND@5	0.0068	0.0103	0.0141	0.0147	0.0138	0.0163	0.0165	0.0192	<u>0.0216</u>	0.0156	0.0164	0.0174	0.0192	0.0268	24.08%
	ND@20	0.0134	0.0186	0.0216	0.0252	0.0232	0.0256	0.0278	0.0307	<u>0.0315</u>	0.0264	0.0309	0.0273	0.0281	0.0383	21.59%
Toys	HR@5	0.0122	0.0121	0.0448	0.0379	0.0638	0.0573	0.0541	0.0631	<u>0.0642</u>	0.0479	0.0515	0.0515	0.0556	0.0747	16.36%
	HR@20	0.0312	0.0290	0.0932	0.0767	0.1285	0.1081	0.1123	<u>0.1277</u>	0.1275	0.1007	0.1112	0.1149	0.0982	0.1339	4.86%
	ND@5	0.0063	0.0077	0.0273	0.0285	0.0379	0.0391	0.0290	0.0371	0.0380	0.0355	0.0338	0.0349	<u>0.0419</u>	0.0541	29.12%
	ND@20	0.0119	0.0123	0.0389	0.0376	0.0563	0.0535	0.0463	0.0559	<u>0.0579</u>	0.0516	0.0511	0.0507	<u>0.0534</u>	0.0707	22.11%
Video	HR@5	0.0165	0.0196	0.0565	0.0568	0.0714	0.0588	0.0621	0.0717	<u>0.0743</u>	0.0566	0.0538	0.0561	0.0613	0.0792	6.59%
	HR@20	0.0493	0.0537	0.1426	0.1386	0.1624	0.1382	0.1563	0.1633	<u>0.1647</u>	0.1394	0.1462	0.1367	0.1423	0.1705	3.52%
	ND@5	0.0097	0.0124	0.0327	0.0339	0.0457	0.0379	0.0461	0.0445	<u>0.0472</u>	0.0342	0.0323	0.0364	0.0412	0.0531	12.50%
	ND@20	0.0191	0.0214	0.0570	0.0579	0.0757	0.0601	0.0705	0.0738	<u>0.0760</u>	0.0584	0.0595	0.0590	0.0639	0.0788	3.68%
ML-1M	HR@5	0.0243	0.0806	0.1097	0.1078	0.1356	0.1492	0.1695	0.1732	<u>0.2055</u>	0.1279	0.1304	0.1489	0.1534	0.2492	21.26%
	HR@20	0.0738	0.2081	0.2689	0.2576	0.3154	0.3413	0.3512	0.3776	<u>0.3698</u>	0.3064	0.3342	0.3283	0.3533	0.4443	20.21%
	ND@5	0.0161	0.0475	0.0669	0.0614	0.0848	0.0977	0.1156	0.1128	<u>0.1396</u>	0.0822	0.0858	0.0993	0.1012	0.1745	24.99%
	ND@20	0.0299	0.0834	0.1143	0.1089	0.1353	0.1518	0.1607	0.1709	<u>0.1813</u>	0.1361	0.1484	0.1492	0.1574	0.2300	26.90%

4.1.4 Implementation Details. For baselines, BPR-MF, GRU4Rec, SASRec, BERT4Rec, and IOCR are implemented using public resources, while other baselines are implemented based on their released codes. All parameters are set based on the values suggested in the original papers and fine-tuned through validation to achieve optimal performance. For InDiRec, we use 2 self-attention layers with attention heads as the sequence encoder, set the batch size to 256, the embedding size d to 64, and the learning rate to 0.001, with Adam [14] as the optimizer. Additionally, τ , m , n , and p are set to 1.0, 4, 50, and 0.1, respectively. λ and γ are chosen from $\{0.2, 0.4, 0.6, 0.8, 1.0\}$, dropout rates from $\{0.1, 0.2, 0.3, 0.4, 0.5\}$, intent prototype size K from $\{32, 64, 128, 256, 512, 1024\}$, diffusion steps T from $\{10, 50, 100, 200, 300, 500\}$, and intent guidance scale ω from $\{0, 1, 2, 3, 4, 5\}$. All methods are trained for 50 epochs with early stopping based on validation results. All experiments are conducted with PyTorch on an NVIDIA GeForce RTX 2080 Ti GPU.

4.2 Overall Performance Comparison

We compared the overall performance of the proposed model, InDiRec, with all baselines across five datasets, as shown in Table 2. The results reveal the following findings:

- Due to its consideration of users' historical interaction information, the RNN-based GRU4Rec is more effective than the non-sequential model BPR-MF. Meanwhile, thanks to the powerful ability of the self-attention mechanism to capture meaningful information from user interaction sequences, SASRec and BERT4Rec consistently outperform BPR-MF and GRU4Rec.
- Compared to the classical models above, contrastive learning-based models perform better. CL4SRec addresses data sparsity through data-level augmentation, while ICLRec and IOCR incorporate user intent for further improvement. Moreover, DuoRec

Table 3: Ablation study on five datasets.

Dataset	Metric	w/o $\mathcal{D}(\cdot)$	w/o IGS	w/o $\mathcal{L}_{\text{diff}}$	w/o \mathcal{L}_{cl}	InDiRec
Beauty	HR@20	0.1063	0.1285	0.0992	0.1267	0.1303
	ND@20	0.0474	0.0650	0.0487	0.0651	0.0662
Sports	HR@20	0.0696	0.0760	0.0744	0.0769	0.0787
	ND@20	0.0313	0.0370	0.0359	0.0377	0.0383
Toys	HR@20	0.1074	0.1313	0.1289	0.1324	0.1339
	ND@20	0.0534	0.0690	0.0668	0.0704	0.0707
Video	HR@20	0.1380	0.1688	0.1640	0.1642	0.1705
	ND@20	0.0614	0.0783	0.0751	0.0755	0.0788
ML-1M	HR@20	0.1686	0.4416	0.4411	0.4373	0.4443
	ND@20	0.0647	0.2242	0.2239	0.2199	0.2300

and MCLRec outperform other baselines by leveraging model-level augmentation to address the representation space distortion caused by data-level augmentation, leading to significant performance improvements. This inspires our idea of intent-enhanced contrastive learning in the representation space.

- Diffusion-based models offer a novel way to improve SR. DiffuASR generates new sequences and appends them to the original, while DreamRec directly generates the next item. However, both models may change the intents of the original sequence or overlook user intent, leading to unsatisfactory performance. CaDiRec generates context-aware sequences with performance comparable to contrastive learning models. DiffuRec performs best among diffusion-based baselines by effectively utilizing latent user interest features and target item guidance.
- Benefiting from intent contrastive learning and the diffusion model, InDiRec significantly outperforms existing models across all metrics on five datasets. Compared to the best baseline, it

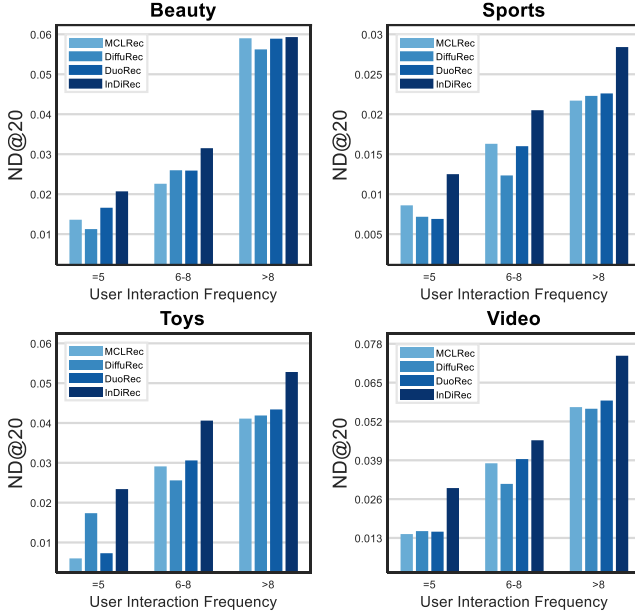


Figure 3: Performance comparison on different user groups.

achieves an average improvement of **13.17%** in HR and **20.68%** in NDCG. This is attributed to InDiRec effectively extracting latent user intents embedded in interaction sequences and using them as guidance signals in the conditional diffusion model to generate intent-aligned positive augmented views for contrastive learning, thereby enhancing SR performance.

4.3 Ablation Study

To validate the effectiveness of each module in InDiRec, we conducted ablation experiments on five datasets, with the results shown in Table 3. Specifically, "w/o $\mathcal{D}(\cdot)$ " refers to the absence of Dynamic Incremental Prefix Segmentation, where we replace it with random augmentation to generate the same amount of data. "w/o IGS" indicates the removal of the intent-guided signal, achieved by setting $\omega=-1$, thereby disabling the guidance. "w/o \mathcal{L}_{diff} " and "w/o \mathcal{L}_{cl} " represent the exclusion of intent-aware diffusion and contrastive learning, respectively, which is implemented by setting their weight coefficients λ and γ to 0. Note that when $\lambda=0$, contrastive learning cannot proceed, so we generate random augmented sequences to replace the sequences generated by diffusion.

From the results we can see that: (1) Compared to using $\mathcal{D}(\cdot)$, random data augmentation not only disrupts the original sequence intent but also causes the model to misinterpret sequence semantics, leading to significant performance degradation, especially on the dense ML-1M dataset. (2) Removing the intent-guided signal results in performance drops across all datasets, indicating that using intent as guidance generates more reasonable augmented views. In contrast, the absence of guidance increases model uncertainty, leading to degraded performance. (3) Replacing intent-aware diffusion with random augmentation for contrastive learning also increases randomness, preventing the backbone SR model from correctly interpreting sequence semantics, and further reducing performance. (4)

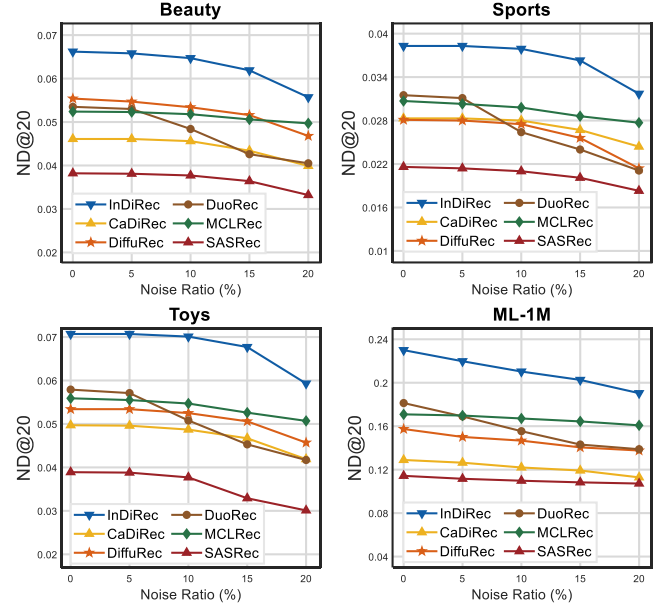


Figure 4: Performance comparison across different noise ratios on four datasets.

Lastly, removing \mathcal{L}_{cl} results in performance degradation, highlighting the importance of contrastive learning [25]. Overall, removing any module reduces InDiRec's performance, which demonstrates the effectiveness of each component.

4.4 Robustness Analysis

4.4.1 Robustness w.r.t. User Interaction Frequency. User cold start is a typical example of the data sparsity problem, where new recommender systems often lack sufficient user interaction data [1]. To evaluate the robustness of InDiRec under such conditions, we split four sparse datasets (Beauty, Sports, Toys, and Video) into three groups based on sequence length and compared InDiRec with strong baseline models. The experimental results are shown in Figure 3. From the figure we can observe that as sequence length decreases, the performance of all models drops significantly, confirming the limitation of data sparsity on recommendation performance. Notably, InDiRec consistently outperforms all strong baselines across datasets and sequence lengths, even in the shortest interaction length (limited to 5), with relatively smaller performance degradation. This demonstrates that InDiRec effectively generates intent-aligned augmented views for contrastive learning, enabling it to maintain strong robustness under varying levels of data sparsity, especially when interactions are limited.

4.4.2 Robustness to Noisy Data. To simulate noise in user behavior data in real-world recommendation scenarios, we randomly add negative items to the sequence during InDiRec's test phase at fixed rates of 5%, 10%, 15%, and 20%, where the percentage denotes the proportion of noise items inserted for the original sequence length. The experimental results are shown in Figure 4. From the figure, we observe that as the noise proportion increases, all models experience varying degrees of performance degradation. Compared to SASRec,

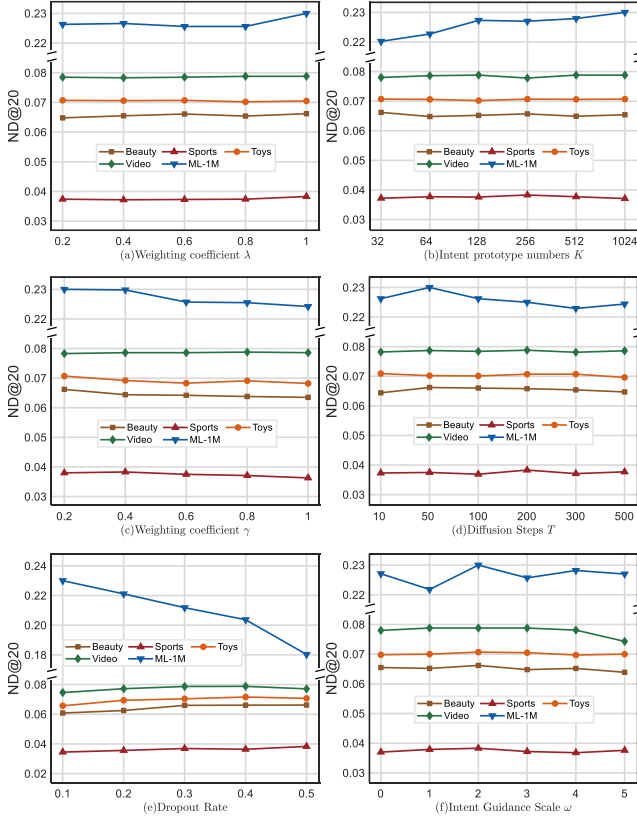


Figure 5: Performance of InDiRec w.r.t. different hyperparameters on NDCG (ND@20), as shown in subfigures (a)-(f).

both DuoRec and MCLRec perform better, which can be attributed to their model-level augmentation that effectively mitigates the randomness caused by data-level noise. Diffusion-based models, such as DiffuRec and CaDiRec, exhibit strong robustness to noise due to their use of diffusion models, which are both noise-sensitive and highly controllable. However, because diffusion models are inherently sensitive to random noise, excessive noise leads to uncertainty in the generated results, causing a more pronounced performance drop when the noise proportion exceeds 15%. Benefiting from the strengths of these models, InDiRec achieves the best performance across various noise levels and datasets. Even with 20% noise, it maintains strong performance, demonstrating that InDiRec can effectively capture user intents and generate reasonable augmented views, which shows strong robustness against noisy data.

4.5 Further Analysis

In this section, we conduct experiments on five datasets to explore how different hyperparameters affect the performance of InDiRec with NDCG (ND@20). In each experiment, we fix all other parameters and tune only one, with the results shown in Figure 5.

4.5.1 Effect of $\mathcal{L}_{\text{diff}}$ and \mathcal{L}_{cl} weight coefficients. InDiRec optimizes its parameters through multi-task learning (Eq.(23)), where λ and γ represent the weight coefficients of the loss functions for intent-aware diffusion $\mathcal{L}_{\text{diff}}$ and contrastive learning \mathcal{L}_{cl} , respectively. As

shown in Figure 5(a) and (c), for λ , all datasets except Toys achieve the best results when set to 1, while for γ , the optimal values vary across datasets. This indicates that intent-aware diffusion is more critical than contrastive learning, and choosing appropriate weights can improve performance. Based on the figure, we set λ to 1 for all datasets except Toys, which is set to 0.2. For γ , we assign 0.4 for Sports, 0.8 for Video, and 0.2 for the remaining datasets.

4.5.2 Effect of the dropout rate. Dropout is a regularization method to mitigate overfitting, and its optimal value depends on dataset characteristics. As shown in Figure 5(e), InDiRec performs best with a dropout of 0.5 on three sparse Amazon datasets, 0.4 on Video, and 0.1 on the dense ML-1M dataset. This indicates that the intent learning of InDiRec is closely related to sequence length: smaller dropout rates cause overfitting on sparse datasets, while larger rates lead to underfitting on dense datasets.

4.5.3 Effect of the intent prototype number K . We define the intent clustering centers obtained by K-means as intent prototypes. Figure 5(b) illustrates the impact of the number of prototypes on performance. The results show that different datasets require varying numbers of intent prototypes, reflecting the diversity of user intent distributions and their dependence on interaction types. Based on the results, we set K to 1024 for Toys and ML-1M, 256 for Sports, 128 for Video, and 32 for Beauty as the default values in InDiRec.

4.5.4 Effect of the diffusion steps T . In this study, T is a key parameter affecting the performance and computational cost of the diffusion model [19]. As shown in Figure 5(d), performance improves with increasing noise scale and reaches a critical point, which varies across datasets. Beyond this point, performance gains slow down and even decline while training time and computational cost increase significantly. This suggests that an overly large T may lead to overfitting and prevent learning intent representations. Based on the results, we set T to 200 for Sports and Toys, 100 for Video, and 50 for Beauty and ML-1M.

4.5.5 Effect of the intent guidance scale ω . We control the strength of the intent-guided signal s_e by adjusting ω , and Figure 5(f) illustrates the impact of different ω values on the performance of InDiRec. From the figure, we observe the following: (1) Higher ω enhances the guidance of intent on the model’s generation direction, improving the generation of personalized intent-aligned views and boosting model performance. (2) However, excessively high ω reduces the diversity of generated results, causing the model to generate views guided by incorrect intents, which further degrades performance. Therefore, selecting an appropriate ω is essential to maximize benefits. Based on the results, all datasets achieve the best performance at $\omega=2$, so we set ω to 2 as the default parameter for InDiRec.

4.6 Visualization of Intent Representation

To analyze the impact of intent information, we visualized generated user sequence representations with and without the intent-guided signal via t-SNE [33] during testing. Figure 6 illustrates examples from the Video and Sports datasets. From the figure, we observe that representations without intent information appear "scattered", while those incorporating intent information are more "close" and

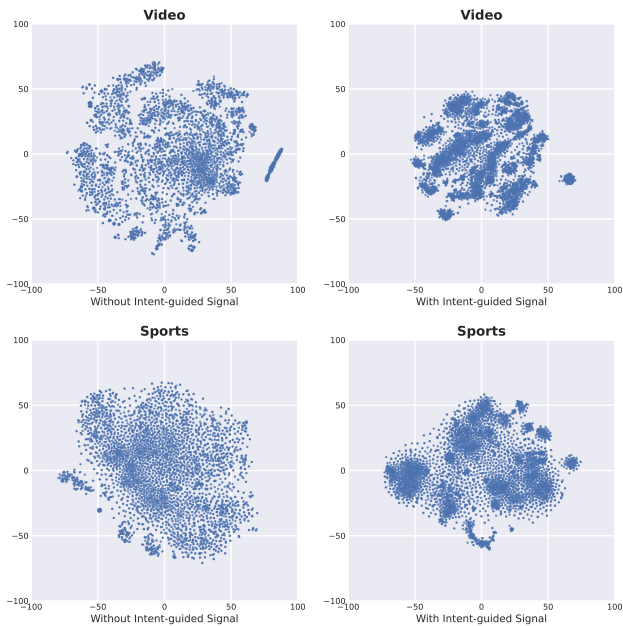


Figure 6: Visualization of learned intent representations.

exhibit clear sub-clusters. The locations and sizes of the intent prototypes vary significantly, indicating that interaction sequences can indeed be categorized into multiple intents, which differ across datasets. In contrast, the dispersed representations without intent information may prevent the model from constructing reasonable positive sample pairs, resulting in collapsed outcomes. By comparison, intent-aware diffusion effectively aggregates sequences with the same intent in the representation space, generating more informative representations based on intent prototypes for contrastive learning, while mitigating over-personalization through classifier-free guidance (See Section 4.5.5), further validating the effectiveness of intent information in representation learning.

5 Related Work

5.1 Sequential Recommendation

Sequential recommendation (SR) predicts the next item a user may interact with based on their historical interactions and has gained significant attention in academia and industry. The early method [27] introduced Markov chains into SR, where the next interaction depends on the previous few interactions. In recent years, with the rise of deep learning, many Deep Learning-based SR models have emerged, such as Recurrent Neural Networks (RNN)-based [9], Convolutional Neural Networks (CNN)-based [31], Graph Neural Networks (GNN)-based [41], and Transformer-based [13, 20, 28, 40] models. However, these models often face challenges from data sparsity and noise in real-world scenarios.

5.2 Contrastive Learning for Recommendation

Contrastive learning has been widely used in deep learning as a powerful self-supervised learning (SSL) approach [3, 4, 24, 39, 46]. Its core focuses on utilizing unlabeled data to generate diverse

supervision signals, improving representation learning. Recently, it has been applied to alleviate the data sparsity issue in SR. S^3 -Rec [46] first introduced contrastive learning to SR through four auxiliary SSL tasks, while CL4SRec [42] and CoSeRec [22] utilized data-level random augmentation to maximize view consistency. Furthermore, GNN-based methods [39, 48] explored the effectiveness of SSL in graph representation learning. Separately, ICLRec [3] and IOCLRec [17] incorporated intent distributions into sequence representations within the contrastive learning framework. To address representation degradation, DuoRec [25] and MCLRec [24] introduced model-level and mixup-level augmentations: the former maintains semantic consistency through neuron dropout, while the latter integrates data-level and model-level augmentations with a learnable augmenter to generate richer contrastive pairs. However, the reliance on random processing in these methods may overlook intent information in the representation space. Moreover, existing methods [3, 17, 29] designed to learn intent representations often fail to construct augmented views consistent with the original sequence semantics, which may result in generating intent-misaligned views, thereby reducing their effectiveness.

5.3 Diffusion Models for Recommendation

Diffusion models (DMs) have demonstrated superior generative capabilities over GANs [8] and VAEs [15] in tasks like image generation [6, 10], text generation [18], and time series imputation [32]. Recently, DMs have been employed in recommender systems to enhance recommendation performance. For instance, CODIGEM [35] and DiffRec [37] first introduced DMs to collaborative filtering. Similarly, some SR methods [7, 19, 38, 44] directly apply the structure of DMs to generate recommended items or sequences. Typical examples include DiffuRec [19] and DreamRec [44], which leverage DMs to learn user interest distributions or generate the next item based on historical interactions as conditional guidance. Other methods [4, 21], such as DiffuASR [21], apply DMs for data augmentation by generating sequences to concatenate with the original sequence for prediction. In contrast, CaDiRec [4] employs context-guided DMs to replace partial items in sequences, generating augmented views for contrastive learning. Unlike existing methods, InDiRec generates synthetic data from a learned intent distribution, producing semantically aligned views as an alternative to heuristic augmentations, and improving SR performance.

6 Conclusion

In this study, we propose an intent-aware diffusion-based contrastive learning model named InDiRec for sequential recommendation. InDiRec generates intent-guided augmented views that enhance the effectiveness of contrastive learning. Extensive experiments on five public benchmark datasets demonstrate its superiority over strong baselines, with further analyses confirming its robustness and semantic consistency. While InDiRec focuses on single-behavior (e.g., purchase) sequences to infer user intents, future work will explore the incorporation of multi-behavior data (e.g., click, cart, favorite), where each behavior type may reflect distinct or evolving user intents. Moreover, we are also interested in exploring potential ethical considerations of InDiRec, such as bias in intent inference and fairness in sequence generation.

References

- [1] Renqin Cai, Jibang Wu, Aidan San, Chong Wang, and Hongning Wang. 2021. Category-aware Collaborative Sequential Recommendation. In *Proceedings of the 44th International ACM SIGIR Conference on Research and Development in Information Retrieval*. 388–397.
- [2] Ting Chen, Simon Kornblith, Mohammad Norouzi, and Geoffrey Hinton. 2020. A simple framework for contrastive learning of visual representations. In *Proceedings of the 37th International Conference on Machine Learning*. 1597–1607.
- [3] Yongjun Chen, Zhiwei Liu, Jia Li, Julian McAuley, and Caiming Xiong. 2022. Intent Contrastive Learning for Sequential Recommendation. In *Proceedings of the ACM Web Conference 2022*. 2172–2182.
- [4] Ziqiang Cui, Haolun Wu, Bowei He, Ji Cheng, and Chen Ma. 2024. Context Matters: Enhancing Sequential Recommendation with Context-aware Diffusion-based Contrastive Learning. In *Proceedings of the 33rd ACM International Conference on Information and Knowledge Management*. 404–414.
- [5] Jacob Devlin, Ming-Wei Chang, Kenton Lee, and Kristina Toutanova. 2019. BERT: Pre-training of Deep Bidirectional Transformers for Language Understanding. In *Proceedings of the 2019 Conference of the North American Chapter of the Association for Computational Linguistics*. 4171–4186.
- [6] Prafulla Dhariwal and Alex Nichol. 2021. Diffusion models beat GANs on image synthesis. In *Advances in Neural Information Processing Systems*. 8780–8794.
- [7] Hanwen Du, Huanhuan Yuan, Zhen Huang, Pengpeng Zhao, and Xiaofang Zhou. 2023. Sequential Recommendation with Diffusion Models. arXiv:2304.04541
- [8] Ian J. Goodfellow, Jean Pouget-Abadie, Mehdi Mirza, Bing Xu, David Warde-Farley, Sherjil Ozair, Aaron C. Courville, and Yoshua Bengio. 2014. Generative Adversarial Nets. In *Advances in Neural Information Processing Systems*. 2672–2680.
- [9] Balázs Hidasi, Alexandros Karatzoglou, Linas Baltrunas, and Domonkos Tikk. 2016. Session-based Recommendations with Recurrent Neural Networks. In *4th International Conference on Learning Representations, ICLR 2016*.
- [10] Jonathan Ho, Ajay Jain, and Pieter Abbeel. 2020. Denoising Diffusion Probabilistic Models. In *Advances in Neural Information Processing Systems*. 6840–6851.
- [11] Jonathan Ho and Tim Salimans. 2022. Classifier-Free Diffusion Guidance. (2022). arXiv:2207.12598
- [12] Jeff Johnson, Matthijs Douze, and Hervé Jégou. 2021. Billion-Scale Similarity Search with GPUs. *IEEE Transactions on Big Data* 7, 3 (2021), 535–547.
- [13] Wang-Cheng Kang and Julian McAuley. 2018. Self-Attentive Sequential Recommendation. In *2018 IEEE International Conference on Data Mining*. 197–206.
- [14] Diederik P. Kingma and Jimmy Ba. 2015. Adam: A Method for Stochastic Optimization. In *International Conference on Learning Representations, ICLR 2015*.
- [15] Diederik P. Kingma and Max Welling. 2014. Auto-Encoding Variational Bayes. In *2nd International Conference on Learning Representations, ICLR 2014*.
- [16] Walid Krichene and Steffen Rendle. 2020. On Sampled Metrics for Item Recommendation. In *Proceedings of the 26th ACM SIGKDD International Conference on Knowledge Discovery and Data Mining*. 1748–1757.
- [17] Xuewei Li, Aitong Sun, Mankun Zhao, Jian Yu, Kun Zhu, Di Jin, Mei Yu, and Ruiguo Yu. 2023. Multi-Intention Oriented Contrastive Learning for Sequential Recommendation. In *Proceedings of the Sixteenth ACM International Conference on Web Search and Data Mining*. 411–419.
- [18] Xiang Li, John Thickstun, Ishaan Gulrajani, Percy S Liang, and Tatsunori B Hashimoto. 2022. Diffusion-LM Improves Controllable Text Generation. In *Advances in Neural Information Processing Systems*. 4328–4343.
- [19] Zihao Li, Aixin Sun, and Chenliang Li. 2023. DiffuRec: A Diffusion Model for Sequential Recommendation. *ACM Transactions on Information Systems* 42, 3, Article 66 (2023), 28 pages.
- [20] Chang Liu, Xiaoguang Li, Guohao Cai, Zhenhua Dong, Hong Zhu, and Lifeng Shang. 2021. Noninvasive self-attention for side information fusion in sequential recommendation. In *Proceedings of the AAAI conference on artificial intelligence*. 4249–4256.
- [21] Qidong Liu, Fan Yan, Xiangyu Zhao, Zhaocheng Du, Huifeng Guo, Ruiming Tang, and Feng Tian. 2023. Diffusion Augmentation for Sequential Recommendation. In *Proceedings of the 32nd ACM International Conference on Information and Knowledge Management*. 1576–1586.
- [22] Zhiwei Liu, Yongjun Chen, Jia Li, Philip S. Yu, Julian McAuley, and Caiming Xiong. 2021. Contrastive Self-supervised Sequential Recommendation with Robust Augmentation. arXiv:2108.06479
- [23] Anjing Luo, Pengpeng Zhao, Yanchi Liu, Fuzhen Zhuang, Deqing Wang, Jiajie Xu, Junhua Fang, and Victor S. Sheng. 2021. Collaborative self-attention network for session-based recommendation. In *Proceedings of the Twenty-Ninth International Joint Conference on Artificial Intelligence*. 2591–2597.
- [24] Xiuyuan Qin, Huanhuan Yuan, Pengpeng Zhao, Junhua Fang, Fuzhen Zhuang, Guanfeng Liu, Yanchi Liu, and Victor Sheng. 2023. Meta-optimized Contrastive Learning for Sequential Recommendation. In *Proceedings of the 46th International ACM SIGIR Conference on Research and Development in Information Retrieval*. 89–98.
- [25] Ruihong Qiu, Zi Huang, Hongzhi Yin, and Zijian Wang. 2022. Contrastive Learning for Representation Degeneration Problem in Sequential Recommendation. In *Proceedings of the Fifteenth ACM International Conference on Web Search and Data Mining*. 813–823.
- [26] Steffen Rendle, Christoph Freudenthaler, Zeno Gantner, and Lars Schmidt-Thieme. 2009. BPR: Bayesian personalized ranking from implicit feedback. In *Proceedings of the Twenty-Fifth Conference on Uncertainty in Artificial Intelligence*. 452–461.
- [27] Steffen Rendle, Christoph Freudenthaler, and Lars Schmidt-Thieme. 2010. Factorizing personalized Markov chains for next-basket recommendation. In *Proceedings of the 19th International Conference on World Wide Web*. 811–820.
- [28] Fei Sun, Jun Liu, Jian Wu, Changhua Pei, Xiao Lin, Wenwu Ou, and Peng Jiang. 2019. BERT4Rec: Sequential Recommendation with Bidirectional Encoder Representations from Transformer. In *Proceedings of the 28th ACM International Conference on Information and Knowledge Management*. 1441–1450.
- [29] Qiaoyu Tan, Jianwei Zhang, Jiangchao Yao, Ninghao Liu, Jingren Zhou, Hongxia Yang, and Xia Hu. 2021. Sparse-Interest Network for Sequential Recommendation. In *Proceedings of the Fourteenth ACM International Conference on Web Search and Data Mining*. 598–606.
- [30] Yong Kiam Tan, Xinxiang Xu, and Yong Liu. 2016. Improved Recurrent Neural Networks for Session-based Recommendations. In *Proceedings of the 1st Workshop on Deep Learning for Recommender Systems*. 17–22.
- [31] Jiayi Tang and Ke Wang. 2018. Personalized Top-N Sequential Recommendation via Convolutional Sequence Embedding. In *Proceedings of the Eleventh ACM International Conference on Web Search and Data Mining*. 565–573.
- [32] Yusuke Tashiro, Jiaming Song, Yang Song, and Stefano Ermon. 2021. CSDI: Conditional Score-based Diffusion Models for Probabilistic Time Series Imputation. In *Advances in Neural Information Processing Systems*. 24804–24816.
- [33] Laurens van der Maaten and Geoffrey Hinton. 2008. Visualizing Data using t-SNE. *Journal of Machine Learning Research* 9, 86 (2008), 2579–2605.
- [34] Ashish Vaswani, Noam Shazeer, Niki Parmar, Jakob Uszkoreit, Llion Jones, Aidan N. Gomez, Lukasz Kaiser, and Illia Polosukhin. 2017. Attention is all you need. In *Advances in Neural Information Processing Systems*. 6000–6010.
- [35] Joojo Walker, Ting Zhong, Fengli Zhang, Qiang Gao, and Fan Zhou. 2022. Recommendation via Collaborative Diffusion Generative Model. In *Knowledge Science, Engineering and Management*. 593–605.
- [36] Shoujin Wang, Liang Hu, Yan Wang, Longbing Cao, Quan Z. Sheng, and Mehmet Orgun. 2019. Sequential Recommender Systems: Challenges, Progress and Prospects. In *Proceedings of the Twenty-Eighth International Joint Conference on Artificial Intelligence*. 6332–6338.
- [37] Wenjie Wang, Yiyan Xu, Fuli Feng, Xinyu Lin, Xiangnan He, and Tat-Seng Chua. 2023. Diffusion Recommender Model. In *Proceedings of the 46th International ACM SIGIR Conference on Research and Development in Information Retrieval*. 832–841.
- [38] Yu Wang, Zhiwei Liu, Liangwei Yang, and Philip S. Yu. 2024. Conditional Denoising Diffusion for Sequential Recommendation. In *Advances in Knowledge Discovery and Data Mining*. 156–169.
- [39] Jiancan Wu, Xiang Wang, Fuli Feng, Xiangnan He, Liang Chen, Jianxun Lian, and Xing Xie. 2021. Self-supervised Graph Learning for Recommendation. In *Proceedings of the 44th International ACM SIGIR Conference on Research and Development in Information Retrieval*. 726–735.
- [40] Liwei Wu, Shuqing Li, Cho-Jui Hsieh, and James Sharpnack. 2020. SSE-PT: Sequential Recommendation Via Personalized Transformer. In *Proceedings of the 14th ACM Conference on Recommender Systems*. 328–337.
- [41] Shu Wu, Yuyuan Tang, Yanqiao Zhu, Liang Wang, Xing Xie, and Tieniu Tan. 2019. Session-based recommendation with graph neural networks. In *Proceedings of the AAAI Conference on Artificial Intelligence*. 346–353.
- [42] Xu Xie, Fei Sun, Zhaoyang Liu, Shiwen Wu, Jinyang Gao, Jiandong Zhang, Bolin Ding, and Bin Cui. 2022. Contrastive Learning for Sequential Recommendation. In *2022 IEEE 38th International Conference on Data Engineering*. 1259–1273.
- [43] Yuhao Yang, Chao Huang, Lianghao Xia, Chunzhen Huang, Da Luo, and Kangyi Lin. 2023. Debaised Contrastive Learning for Sequential Recommendation. In *Proceedings of the ACM Web Conference 2023*. 1063–1073.
- [44] Zhengyi Yang, Jiancan Wu, Zhicai Wang, Xiang Wang, Yancheng Yuan, and Xiangnan He. 2023. Generate What You Prefer: Reshaping Sequential Recommendation via Guided Diffusion. In *Advances in Neural Information Processing Systems*. 24247–24261.
- [45] Junliang Yu, Hongzhi Yin, Xin Xia, Tong Chen, Jundong Li, and Zi Huang. 2024. Self-Supervised Learning for Recommender Systems: A Survey. *IEEE Transactions on Knowledge and Data Engineering* 36, 1 (2024), 335–355.
- [46] Kun Zhou, Hui Wang, Wayne Xin Zhao, Yutao Zhu, Sirui Wang, Fuzheng Zhang, Zhongyuan Wang, and Ji-Rong Wen. 2020. S3-Rec: Self-Supervised Learning for Sequential Recommendation with Mutual Information Maximization. In *Proceedings of the 29th ACM International Conference on Information and Knowledge Management*. 1893–1902.
- [47] Peilin Zhou, Jingqi Gao, Yueqi Xie, Qichen Ye, Yining Hua, Jaeboum Kim, Shoujin Wang, and Sunghun Kim. 2023. Equivariant Contrastive Learning for Sequential Recommendation. In *Proceedings of the 17th ACM Conference on Recommender Systems*. 129–140.
- [48] Yanqiao Zhu, Yichen Xu, Feng Yu, Qiang Liu, Shu Wu, and Liang Wang. 2021. Graph Contrastive Learning with Adaptive Augmentation. In *Proceedings of the ACM Web Conference 2021*. 2069–2080.